Cell Calcium 87 (2020) 102181

Contents lists available at ScienceDirect

Cell Calcium

journal homepage: www.elsevier.com/locate/ceca

Divalent cation influx and calcium homeostasis in germinal vesicle mouse oocytes

Goli Ardestani[a], Aujan Mehregan[a,1], Andrea Fleig[b], F. David Horgen[c], Ingrid Carvacho[d], Rafael A. Fissore[a,*]

[a] Department of Veterinary and Animal Sciences, University of Massachusetts Amherst, 661 North Pleasant Street, Amherst, MA, 01003, USA
[b] Center for Biomedical Research at The Queen's Medical Center and University of Hawaii Cancer Center and John A. Burns School of Medicine at the University of Hawaii, Honolulu, HI, 96813, USA
[c] Department of Natural Sciences, Hawaii Pacific University, Kaneohe, HI, 96744, USA
[d] Department of Biology and Chemistry, Faculty of Basic Sciences, Universidad Católica del Maule, 3480112, Talca, Chile

ARTICLE INFO

Keywords:
Calcium
Influx
Signaling
TRPV3
TRPM7
Cav3.2
Meiosis

ABSTRACT

Prior to maturation, mouse oocytes are arrested at the germinal vesicle (GV) stage during which they experience constitutive calcium (Ca^{2+}) influx and spontaneous Ca^{2+} oscillations. The oscillations cease during maturation but Ca^{2+} influx continues, as the oocytes' internal stores attain maximal content at the culmination of maturation, the metaphase II stage. The identity of the channel(s) that underlie this Ca^{2+} influx has not been completely determined. GV and matured oocytes are known to express three Ca^{2+} channels, $Ca_V3.2$, TRPV3 and TRPM7, but females null for each of these channels are fertile and their oocytes display minor modifications in Ca^{2+} homeostasis, suggesting a complex regulation of Ca^{2+} influx. To define the contribution of these channels at the GV stage, we used different divalent cations, pharmacological inhibitors and genetic models. We found that the three channels are active at this stage. $Ca_V3.2$ and TRPM7 channels contributed the majority of Ca^{2+} influx, as inhibitors and oocytes from homologous knockout (KO) lines showed severely reduced Ca^{2+} entry. Sr^{2+} influx was promoted by $Ca_V3.2$ channels, as Sr^{2+} oscillations were negligible in *$Ca_V3.2$*-KO oocytes but robust in control and *Trpv3*-KO GV oocytes. Mn^{2+} entry relied on expression of $Ca_V3.2$ and TRPM7 channels, but Ni^{2+} entry depended on the latter. $Ca_V3.2$ and TRPV3 channels combined to fill the Ca^{2+} stores, although $Ca_V3.2$ was the most impactful. Studies with pharmacological inhibitors effectively blocked the influx of divalent cations, but displayed off-target effects, and occasionally agonist-like properties. In conclusion, GV oocytes express channels mediating Ca^{2+} and other divalent cation influx that are pivotal for fertilization and early development. These channels may serve as targets for intervention to improve the success of assisted reproductive technologies.

1. Introduction

A wide range of cellular processes such as gene expression, muscle contraction, secretion, cell division, fertilization and apoptosis are regulated by changes in the intracellular concentration of free calcium ($[Ca^{2+}]_i$) [1]. To accomplish this, cells devote significant amounts of their energy reserves to create and maintain Ca^{2+} gradients between the extracellular and intracellular environments as well as between cellular compartments such that brief changes in $[Ca^{2+}]_i$ can have profound signaling effects [2].

Transient rises in $[Ca^{2+}]_i$ as well as Ca^{2+} influx from the extracellular environment ($[Ca^{2+}]_o$) play important roles in unfertilized and fertilized oocytes in all animal species from marine invertebrates to mammals [3–5]. In mammals, $[Ca^{2+}]_i$ rises in MII oocytes, henceforth called eggs, induce exit from the meiotic arrest triggering egg activation and initiation of embryo development [6]. Prior to this stage, changes in Ca^{2+} homeostasis also occur during maturation, including spontaneous oscillations at the GV stage, and accumulation of Ca^{2+} in the endoplasmic reticulum (ER), the main internal Ca^{2+} store ($[Ca^{2+}]_{ER}$) [7]. The function of these Ca^{2+} changes prior to fertilization is not well established, although Ca^{2+} content in the ER is necessary to support the protein synthesis required for meiosis progression, and for the initial $[Ca^{2+}]_i$ rises post fertilization [8,9]. Remarkably, even though extracellular Ca^{2+} underlies both the spontaneous oscillations and the filling

* Corresponding author.
E-mail address: rfissore@vasci.umass.edu (R.A. Fissore).
[1] Present address: Department of Cellular and Molecular Medicine, KU Leuven, Herestraat 49 – PB601, 3000 Leuven, Belgium.

https://doi.org/10.1016/j.ceca.2020.102181
Received 19 September 2019; Received in revised form 11 February 2020; Accepted 11 February 2020
Available online 12 February 2020

of $[Ca^{2+}]_{ER}$ stores [10–12], the plasma membrane (PM) channel(s) that underpin Ca^{2+} influx at GV stage have remained uncharacterized.

Cells have at their disposal multiple PM channel(s) and transporters to maintain Ca^{2+} homeostasis [11,13]. Oocytes and eggs are not an exception, and divalent cation permeable PM channel(s) were detected early on in these cells using electrophysiology [14,15]. It was noted that voltage-dependent Ca^{2+} currents were present in GV oocytes and in MII eggs [16,17], and that the presence of this current was associated with acquisition of meiotic competence [15]. Predictably, $Ca_V3.2$ (member of the T-type Cav sub-group [18]), which are voltage gated Ca^{2+} channels, were the first channels whose functional expression was demonstrated in eggs and zygotes [19,20]. Although readily detectable, genetic studies found that mice lacking $Ca_V3.2$ are fertile and their oocytes and eggs display only slightly reduced $[Ca^{2+}]_{ER}$ content [21]. Importantly, how $Ca_V3.2$ channels affected spontaneous oscillations or divalent cation plasma membrane fluxes in GV oocytes and during maturation was not examined.

Given that *$Ca_V3.2$*-KO mice are fertile, other Ca^{2+} influx mechanism (s) must be functional in mammalian oocytes and eggs. A proposed mechanism of Ca^{2+} influx was the Store Operated Ca^{2+} Entry (SOCE), which is composed of STIM1, that acts as the sensor of ER Ca^{2+} levels, and ORAI1, which is the PM channel [22,23]. Although STIM1 and ORAI1 appear to be expressed at the molecular level in mouse oocytes [10], the functional expression of ORAI1 via electrophysiology has not been confirmed, and single or combined genetic deletion of *Stim1/2* and *Orai1* failed to affect Ca^{2+} influx in mouse oocytes and/or eggs [24]. The transient receptor potential (TRP) family of channels could also mediate Ca^{2+} influx in mouse oocytes and eggs. TRP channels are grouped into six subfamilies: TRPC, TRPM, TRPV, TRPA, TRPML, and TRPP (or PKD) [25,26]. These channels are, in general, nonselective, weakly voltage-dependent, and display widespread expression. We have previously reported functional expression of TRPV3 and TRPM7 in mouse oocytes and eggs [27,28], and showed that they are under distinct regulation during oocyte maturation. For example, TRPV3 expression was undetectable by electrophysiology at the GV stage, but its activity increased gradually during maturation and peaked at the MII stage [27]. It was not examined however if TRPV3 impacts $[Ca^{2+}]_{ER}$ content in GV oocytes, and whether it mediates entry of other divalent cations at this stage. Importantly, just like *$Ca_V3.2$* null mice, *Trpv3*-KO mice are fertile [27]. Unlike TRPV3, the functional expression of TRPM7 is more prominent in GV oocytes than in MII eggs, and its functional expression experiences a rebound after fertilization in 2-cell embryos [28]. Whole-animal deletion of *Trpm7* is embryonically lethal, which has prevented the study of its function in gametes of *Trpm7*-null mice. However, a recently generated conditional allele showed that TRPM7 mediates Ca^{2+} influx in GV oocytes and in eggs post-fertilization, although conditional KO (cKO) females displayed normal fertility [29]. TRPM7 displays permeability to a range of trace metal ions [30] including Mg^{2+} and Zn^{2+}. It has been shown that Zn^{2+} plays a critical role in oocyte maturation and fertilization [31]. Therefore, it cannot be ruled out that besides permeating Ca^{2+}, this channel plays a primary role in permeating other divalent cations in mouse oocytes and eggs [28].

In this study, we used a combination of techniques including fluorescence imaging, genetic models and pharmacological agents to identify the contribution of the three known channels to divalent cation influx in mouse GV oocytes. We aimed to determine their preference for specific divalent cations measured by fluorescence, establish their contributions to $[Ca^{2+}]_{ER}$ content, and test the specificity of commonly used pharmacological inhibitors. We found that all three channels $Ca_V3.2$, TRPV3, and TRPM7 are active at this stage, although $Ca_V3.2$ and TRPM7 are largely responsible for Ca^{2+} influx. These channels supply the $[Ca^{2+}]_{ER}$ of GV oocytes, albeit $Ca_V3.2$ seems the most important. Lastly, multiple divalent cations pass through these channels, but not to the same extent, as determined by the inability of certain divalent cations to induce intracellular responses in oocytes from KO models and/or in the presence of inhibitors, some of which displayed off-target effects and/or agonist-like properties.

2. Materials and methods

2.1. Mouse strains and collection of mouse oocytes

$Ca_V3.2$-KO mice were purchased from Jackson Laboratory JAX stock #013770; Bar Harbor, ME [32]. *Trpv3*-KO mice with mixed background of C57BL/6 and 129/SvEvTac, were the generous gift from Dr. Cheng (University of Michigan, Ann Arbor, MI) [33]. To generate *Trpv3-$Ca_V3.2$*-KO (double knockout) colony, single KO mice were mated together. Double heterozygotes males and females mated to achieve double knockout animals. CD1 females and WT C57BL/6 females were used as controls.

GV oocytes were collected from ovaries of 6- to 10-week-old female mice 44–46 h after injection of 5 IU of pregnant mare serum gonadotropin (PMSG; Sigma; Saint Louis, MO). Immediately after euthanasia, MII eggs were collected from the oviducts (CD1 females) 12–14 h after administration of 5 IU of human chorionic gonadotropin (hCG), which was administered 46–48 h after PMSG. Cumulus cells were removed with 0.1 % bovine testes hyaluronidase (Sigma). HEPES–buffered Tyrode's lactate solution (TL-HEPES) containing 5% heat-treated fetal calf serum (FCS; Gibco/ThermoFisher; Waltham, MA) and 100 μM IBMX was used to collect cumulus intact GV oocytes. Cumulus cells were removed by repetitive pipetting and denuded oocytes were kept in Chatot, Ziomek, and Bavister (CZB) media supplemented with 3 mg/ml bovine serum albumin (BSA) and IBMX and were incubated under mineral oil at 37 °C in a humidified atmosphere of 5% CO_2. All animal procedures were performed according to research animal protocols approved by the University of Massachusetts Institutional Animal Care and Use Committee.

2.2. PCR genotyping

PCR genotyping were performed using ear punch samples to confirm *Trpv3*-KO line, using primers as previously described [33]. Jackson Laboratory protocol was followed to confirm *$Ca_V3.2$*-KO line [32]. Both sets of primers were used to confirm *Trpv3-$Ca_V3.2$*-KO line.

2.3. Total RNA extraction and real time PCR

High Pure RNA Isolation Kit (11828665001; Roche Life Sciences) was used to extract total RNA from GV oocytes (n = 50) and MII eggs (n = 50) of CD1 females. iScript cDNA Synthesis kit (1708890; Bio Rad) was used for cDNA synthesis. Taqman qPCR was performed using gene expression assays to detect the three ion channels in both GV oocytes and MII eggs using following primers: TRPV3 (Mm00455003_m1), TRPM7 (Mm00457998_m1), $Ca_V3.2$ (Mm00445382_m1) (ThermoFisher SCIENTIFIC).

2.4. Western blot

Mouse GV oocytes and MII eggs (n = 200 or 400) were collected from CD1 females as described above. Whole lysates were prepared by the immediate addition of 2X-Laemmli sample buffer and frozen at −80 °C until use. Whole tissue lysates were prepared as previously described by our laboratory (Wu et al., 1998, and He et al., 1997). Thawed samples were boiled for 3 min, mixed well and loaded onto 5.0-% SDS-PAGE gels, and the resolved polypeptides were transferred onto Nitrocellulose membranes (FisherScientific, Cat # 45-004-002) using a Mini Trans-Blot Cell (Bio-Rad, Hercules, CA). Transfer was done using transfer buffer (4X) without methanol. The membranes were blocked in 6% nonfat dry milk in PBS– 0.1 % Tween, and incubated overnight at 4 °C with the selected primary antibody; this was followed by multiple washes and finally for 1 h of incubation with a horseradish

peroxidase–labeled secondary antibody (BioRad, Cat # 170-6515, 1:2000). Immunoreactivity was detected using chemiluminescence reagents (NEN Life Science Products, Boston, MA) and visualized using a G-box imaging system (Syngene). The primary antibodies were a rabbit anti-TRPM7 monoclonal (Abcam, Cat # EPR4582, 1:1000 dilution); a rabbit anti-$Ca_V3.2$ polyclonal antibody (Alomone, Cat # ACC-025, 1:500); and an anti-TRPV3 (N15/4) (Neuromab Cat # 75-043). Western blots were repeated at least two times.

2.5. Imaging procedures and monitoring of divalent cation influx

Ca^{2+} imaging was performed as previously described by our laboratory [34], using a Ca^{2+} sensitive dye Fura-2-acetoxymethyl ester (Fura 2-AM, Invitrogen/ThermoFisher). Oocytes were loaded with 1.25 μM Fura-2AM supplemented with 0.02 % Pluronic acid (Invitrogen) for 20 min at room temperature (RT). Oocytes were placed in micro-drops of TL-HEPES on glass bottom dish (Mat-Tek Corp., Ashland, MA) under mineral oil. Oocytes were monitored simultaneously using an inverted microscope (Nikon, Melville, NY) outfitted for fluorescence measurements. Fura 2-AM was excited between 340 and 380 nm wavelengths using a 75 W Xenon arc lamp and a filter wheel (Ludl Electronic Products Ltd., Hawthorne, NY), and fluorescence was captured every 20 s. The emitted light above 510 nm was collected by a cooled Photometrics SenSys CCD camera (Roper Scientific, Tucson, AZ). Nikon Element software was used to coordinate the filter wheel and data acquisition. The acquired data were saved and analyzed using Microsoft Excel and GraphPad Prism Version 5.0 (GraphPad Software, La Jolla, CA). Ca^{2+} influx and spontaneous Ca^{2+} oscillations were measured using TL-HEPES media containing the standard concentration of 2 mM $CaCl_2$. We also induced Ca^{2+} influx and oscillations by adding extra Ca^{2+} to a final concentration of 5 mM, 10 min after the initiation of Ca^{2+} monitoring. Assessment of Sr^{2+} influx and oscillations were carried out in Ca^{2+} free TL-HEPES supplemented with 10 mM Sr^{2+} throughout the monitoring period. Mn^{2+} influx studies were performed in TL-HEPES media containing 2 mM $CaCl_2$, which 100 μM Mn^{2+} were added 5 min after the initiation of monitoring. Mn^{2+} influx was estimated by the quenching of Fura-2′s fluorescence intensity at the 360 nm wavelength, which is the isosbestic point. To detect Ni^{2+} influx, oocytes were loaded with 0.5 μM Mag-Fura-2AM (Invitrogen) supplemented with 0.02 % Pluronic acid for 10 min at RT. Monitoring of Ni^{2+} influx, which caused a decrease in the intensity of Mag-Fura-2 at both wavelengths was performed in nominal Divalent Free Media (DFM, nominal Ca^{2+} and Mg^{2+} free TL-HEPES). Mag-Fura-2 was excited as for Fura-2 and fluorescence captured every 20 s. Ca^{2+} influx studies following emptying of the stores by thapsigargin (TG) were performed in nominal Ca^{2+} free TL-HEPES. Ca^{2+} was added to a final concentration of 5 mM at the indicated time point several minutes after the initial Ca^{2+} rise caused by TG, had reached baseline values.

2.6. Measurement of Ca^{2+} store content

GV oocytes were kept in CZB media supplemented with IBMX and 0.01 % polyvinyl alcohol (PVA; Sigma) at 37 °C in a humidified atmosphere of 5% CO_2 for 1 h in the presence of specific inhibitors. The specific inhibitors were kept during loading of Fura-2AM and Ca^{2+} monitoring. Emptying of the stores was performed in nominal Ca^{2+} free TL-HEPES following the addition of Ionomycin (IO) (2.5 μM) or thapsigargin (10 μM) at the indicated time points. Amplitude and area under the curve (AUC) of Ca^{2+} rise was assessed.

2.7. Pharmacological agents

NS8593 (N2538), $NiCl_2.6H_2O$ (N6136) and $MgCl_2.6H_2O$ (M2393) were purchased from Sigma Aldrich. Mibefradil (2198) was from Tocris. 2-APB (100065), Thapsigargin (586005) and Ionomycin (407592) were from Calbiochem. Waixenicin A was provided as a generous gift from Dr. F. David Horgen, Hawaii Pacific University, Kaneohe, HI. Stock solutions were made following manufacturers' recommendations and kept in -80 °C.

2.8. Slope calculations

The slope of the decline of the fluorescence intensity caused by the addition of Mn^{2+} and Ni^{2+} was used to estimate the influx of these ions. The rate of quenching (ΔF360 and ΔF380) was measured by analyzing the slope of the fluorescence decline for 4 min between X_1: the first value after addition of the divalent cation where noticeable quenching was observed, and X_2: the value after 4 min had elapsed from X1. ΔF360 and ΔF380 was normalized relative to the fluorescence level at inflection point. This method was chosen as it permitted to compare the effects of all the inhibitors on the rate of influx of Mn^{2+} and Ni^{2+} influx with a single slope. Corresponding values for each oocyte were collected, averaged and statistically compared.

2.9. Statistical analysis

Values from at least three different experiments were used for evaluation of statistical significance for each of the comparisons performed. The Prism software (GraphPad Software) was used to perform the statistical comparisons using Student's *t*-test or one-way ANOVA or Chi Square test, according to the experiment analyzed. All bar graphs are presented as mean ± SEM. Significant differences were considered at P values < 0.05.

3. Results

3.1. Assessing divalent cation influx in GV oocytes

Mouse GV oocytes display spontaneous oscillations in the presence of $[Ca^{2+}]_o$ or $[Sr^{2+}]_o$ [7,35], which suggests the expression of non-selective cation channel(s) in these cells. This is in agreement with reports describing functional expression in oocytes and/or eggs of $Ca_V3.2$ and TRPM7 channels, which are all capable of permeating a variety of divalent cations [21,24,27,29]. However, whether the level of expression of Cav3.2 and TRPM7 channels change during maturation, and which or if all these channel(s) are responsible for the influx of divalent cations in GV oocytes is unknown. To gain insight into these questions, we tested the expression of the channels in GV oocytes and MII eggs. We first used quantitative reverse transcriptase PCR, and our results show that the expression of these channels does not change between these stages (Supp. Fig. 1). Next, we performed western blotting with commercially available antibodies and whole cell lysates containing between 200–400 oocytes/eggs. A prominent immunoreactive band corresponding to TRPM7, approximate MW of 220 kDa (Fig. 1A), was observed in oocyte and eggs, whereas we failed to detect immunoreactivity for the other two channels in these cells (Supp. Fig. 2A and data not shown). Remarkably, the TRPM7 levels seemed to increase during maturation, and its relative MW in MII eggs appeared higher than in GV oocytes, which suggests that TRPM7 undergoes phosphorylation during this process. The antibody used to detect TRMP7, was also reactive against TRPM6. Whereas we detected TRPM6 prominently in three different tissues (Fig. 1B), we did not detect it in oocytes and/or eggs (Fig. 1A), in agreement with previous reports [28], although a faint band corresponding to TRPM7 was apparent in the kidney lane (Fig. 1B). Brain showed immunoreactivity against $Ca_v3.2$ (Suppl. Fig. 2B), although immunoreactivity to TRPV3 was difficult to judge due to many non-specific bands (data not shown); noteworthy, TRPV3 expression in eggs was previously reported by us using electrophysiology and immunofluorescence [27]. It is worth noting that $Ca_V3.2$ has been functionally tested by Ca^{2+} imaging and electrophysiology in MII eggs [21].

Given the higher sensitivity of Ca^{2+} imaging to detect functional

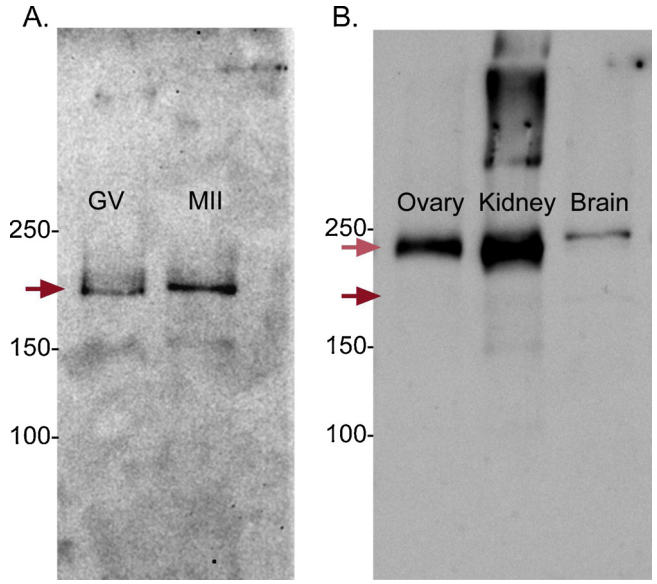

Fig. 1. TRPM7 protein is expressed in mouse GV oocytes and MII eggs. Immunoreactivity of TRPM7 was detected using an anti-TRPM7 + TRPM6 antibody. **(A)** The immunoreactive band in oocytes and eggs is likely TRPM7 given the ~MW of 220 kDa, and because its functional expression was confirmed by electrophysiology [28]. **(B)** In all tissues tested here, TRPM6 expression (~MW 240 kDa) appears to be clearly predominant over TRPM7. Red arrows indicate the expected locations of TRPM7 (dark red) and TRPM6 (light red). Representative blots are shown.

expression of channels vs. western blotting, and the need to ascertain the active channels in GV oocytes, we used this approach to probe the active channels in oocytes. We monitored the influx of various divalent cations besides Ca^{2+} and Sr^{2+} such as Mn^{2+} and Ni^{2+}. Mn^{2+} has been widely used to test divalent influx in cells and eggs [36,37], whereas Ni^{2+}, which effectively inhibits voltage-gated Ca^{2+} channels especially $Ca_V3.2$ [38], efficiently permeates through TRPM7 [30]. We used fluorometric dyes to monitor the influx of these cations [39]. Our results show that all the aforementioned divalent cations persistently enter the ooplasm. The influx of Ca^{2+} and Sr^{2+} induced oscillations, although of different frequencies (Fig. 2A, B), while Mn^{2+} and Ni^{2+} caused sustained fluorescence quenching (Fig. 2C, D). In addition, whereas Ca^{2+}, Sr^{2+}, and Mn^{2+} gained rapid access into the ooplasm, Ni^{2+} required several min (Fig. 2D). These results show that the PM of GV oocytes is permeable to multiple divalent cations, and suggest that the level(s) of expression and function of the underlying channels is closely regulated.

3.2. Several channels contribute to spontaneous and induced Ca^{2+} influx in GV oocytes

We next examined which of the aforementioned PM channels underlies the spontaneous $[Ca^{2+}]_i$ oscillations in GV oocytes. For this we first used oocytes from mice null for specific channels. We tested $[Ca^{2+}]_i$ oscillations in oocytes from *$Ca_V3.2$*, *Trpv3* and *Trpv3-$Ca_V3.2$* null mice (see Materials and Methods). We found that *Trpv3*-KO oocytes showed spontaneous oscillations similar to those of WT and CD1 oocytes, whereas fewer oocytes from *$Ca_V3.2$* and *Trpv3-$Ca_V3.2$*-KO mice exhibited oscillations, which also were of much shorter duration (Fig. 3A). These results suggest that expression of $Ca_V3.2$ channels is necessary to support the spontaneous Ca^{2+} oscillations in GV oocytes (Fig. 3D; $P < 0.5$).

Ca^{2+} influx can be abruptly induced in GV oocytes, and we therefore examined if this type of influx was mediated by the same channel (s). To accomplish this we used two well established methods [40]: first, we raised $[Ca^{2+}]_o$ from 2 mM to 5 mM, and second, after emptying the stores with TG, we raised $[Ca^{2+}]_o$ from 0 mM to 5 mM. Baseline $[Ca^{2+}]_i$ levels were monitored prior to increasing $[Ca^{2+}]_o$, and monitoring continued after the addition of Ca^{2+}. We found that raising $[Ca^{2+}]_o$ stimulated Ca^{2+} influx in oocytes of all strains (Fig. 3B, E), although with slightly greater initial rise (amplitude) and persistence in WT, *Trpv3,* and *Trpv3-$Ca_V3.2$*-KO oocytes than in oocytes of *$Ca_V3.2$*-KO mice. Significant differences were detected when applying the TG protocol (Fig. 3C); we observed a time delay to the first $[Ca^{2+}]_i$ rise in both *$Ca_V3.2$*- and *Trpv3-$Ca_V3.2$*-KO oocytes (Fig. 3F; $P < 0.05$), and in *$Ca_V3.2$*-KO oocytes $[Ca^{2+}]_i$ levels quickly returned to the original baseline values, which was not the case for oocytes of the other strains that continued to oscillate above the baseline. These results suggest that $Ca_V3.2$ channels play an important role in the influx of Ca^{2+} in GV oocytes, although other channels, especially following abrupt increases, are also involved in Ca^{2+} entry in these cells. How $Ca_V3.2$ channels participate in this influx is unknown, but it is possible that they mediate an initial influx of Ca^{2+} that causes changes in membrane potential

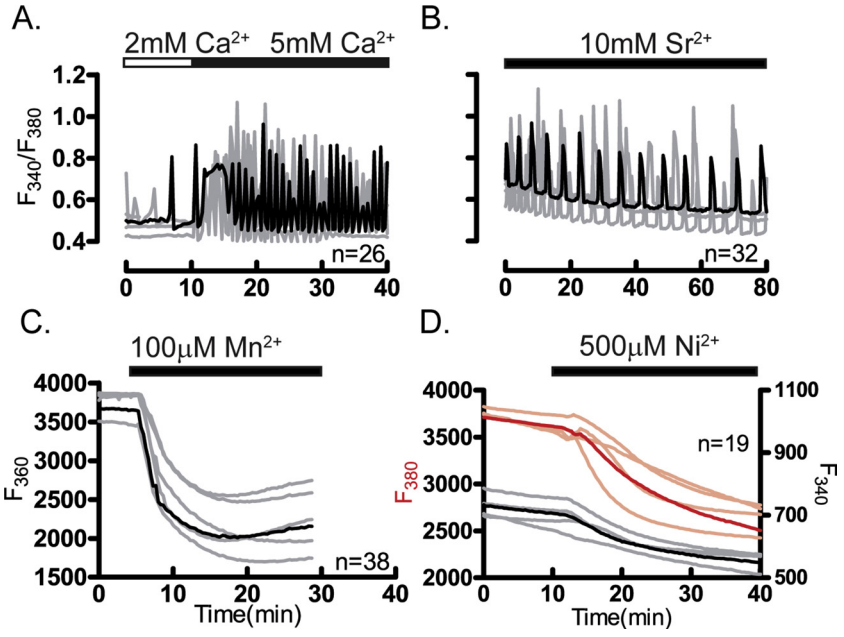

Fig. 2. Divalent cations permeate the plasma membrane of GV oocytes. Divalent cation influx was examined in GV oocytes. **(A)** Representative traces of Ca^{2+} oscillations caused by enhanced influx after increasing $[Ca^{2+}]_o$ from 2 mM to 5 mM. **(B)** Sr^{2+} induced oscillations. **(C)** Fluorescence quenching at F360 following Mn^{2+} addition (100 μM). **(D)** Fluorescence quenching at F380 following Ni^{2+} addition (500 μM) in oocytes loaded with Mag-Fura-2AM in DFM media. Horizontal bars above each panel show the time during which divalent cations were added to the media. All experiments were replicated 4 times. In all panels in this figure and throughout the manuscript, representative traces are shown; darker traces represent the most common response; n: total number of oocytes examined.

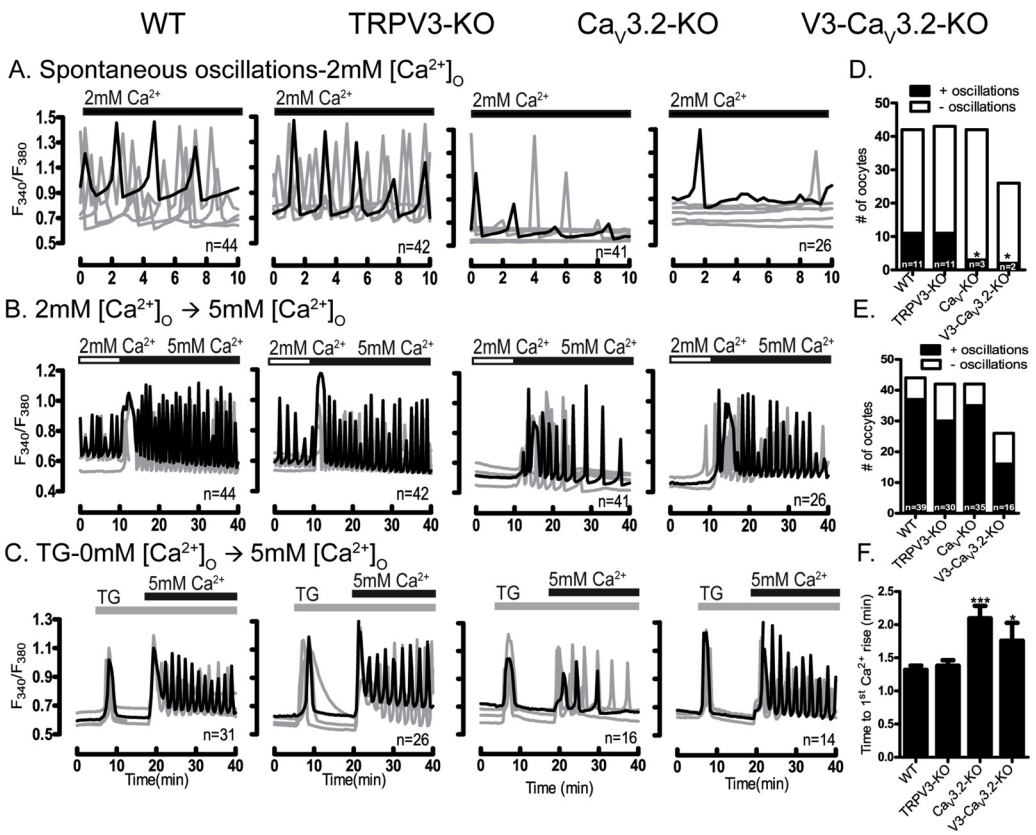

Fig. 3. Ca^{2+} influx in GV oocytes is mediated by multiple channels. Presence of spontaneous oscillations and Ca^{2+} influx examined in WT oocytes and oocytes lacking TRPV3, $Ca_V3.2$ & V3-$Ca_V3.2$ channels. **(A**-four upper panels**)** Spontaneous Ca^{2+} oscillations in WT and KO oocytes in media containing basal Ca^{2+} levels (2 mM). Fewer oocytes of the $Ca_V3.2$ and V3-$Ca_V3.2$ KO lines display oscillations, which are also of decreased frequency **(D)** ($P < 0.05$). **(B**-four medium panels**)** Ca^{2+} influx triggered by increasing $[Ca^{2+}]_o$ from 2 mM to 5 mM induces oscillations in all WT and KO lines, which appear of equal initial frequency **(E)**. **(C**-four lower panels**)** After addition of TG (10 μM), Ca^{2+} influx resulted in reduced responses in $Ca_V3.2$ and V3-$Ca_V3.2$ KO oocytes, especially in the interval from Ca^{2+}addition to the 1st Ca^{2+} peak ($P < 0.05$) **(F)**. Filled horizontal bars above each panel show the time of addition of Ca^{2+} (black) or TG (grey) to the media. All experiments were 4 replicated for times. Asterisk(s) above columns in bar graphs denote significant differences from other conditions here and throughout the manuscript.

and/or activate nearby channels triggering the opening of these Ca^{2+} channels that are ultimately responsible for the large influx, but these possibilities remain to be established.

To identify the channel(s) capable of mediating the remaining influx associated with abrupt Ca^{2+} increases, we made use of pharmacological inhibitors (see Suppl. Table 1 for summary of inhibitors and suggested specificity). We first examined the effects of common $Ca_V3.2$ channel inhibitors such as Mibefradil (1μM) and Ni^{2+} (100μM) [41]. These inhibitors failed to prevent the initiation of oscillations following addition of extra $[Ca^{2+}]_o$, confirming that Ca^{2+} can permeate through other channel(s) (Fig. 4A, B). It is worth noting that whereas mibefradil eventually terminated the oscillations, Ni^{2+} had negligible effect and it might have slightly prolonged the responses. We next examined the participation of TRPM7 channels, as we have previously shown that its inhibition abrogated Ca^{2+} influx in GV oocytes [28]. We first used two general inhibitors: 2-APB (50 μM) and $MgCl_2$ (10 mM). These inhibitors prevented oscillations, although $MgCl_2$ was more effective (Fig. 4C). We then examined more specific inhibitors of TRPM7, and showed that

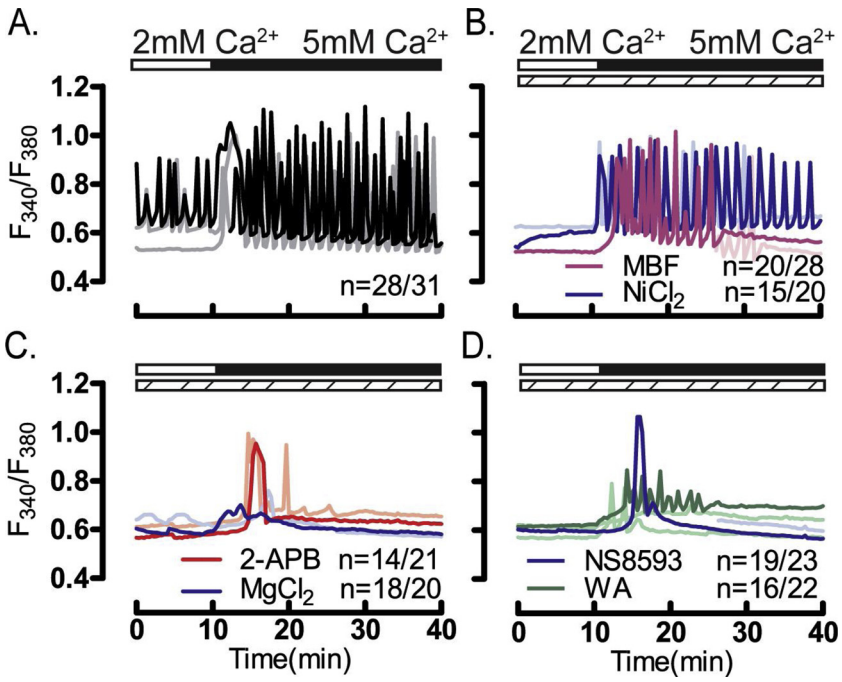

Fig. 4. Pharmacological inhibitors disrupt Ca^{2+} influx/oscillations in GV oocytes. Ca^{2+} influx in GV oocytes was tested by increasing $[Ca^{2+}]_o$ from 2- to 5 mM (white/black horizontal bars above each panel) in the presence of pharmacological inhibitors (dashed bars). Increasing $[Ca^{2+}]_o$ in **(A)** control, untreated oocytes, or oocytes treated with **(B)** $Ca_V3.2$ inhibitors: MBF (1 μM) or Ni^{2+} (100 μM) induced oscillations in the majority of oocytes. Conversely, Increasing $[Ca^{2+}]_o$ in the presence of the **(C)** general TRP channel inhibitors 2-APB (50 μM) or $MgCl_2$ (10 mM), or **(D)** in the presence of the TRPM7 inhibitors NS8593 (10 μM) or waixenicin-A (5 μM) failed to induce oscillations ($P < 0.05$). All experiments were performed in 4 replicates.

NS8593 (10 μM) had a strong inhibitory effect (Fig. 4D), which is consistent with our previous results [28]. We also used waixenicin-A (WA, 5 μM), which purportedly has the highest specificity against TRPM7 [42,43]; WA also effectively suppressed Ca^{2+} influx and oscillations (Fig. 4D). We repeated these studies using the TG approach (Suppl. Fig. 3). Our results were mostly consistent with the previous data in that $Ca_V3.2$ inhibitors were ineffective at reducing the initial Ca^{2+} influx, and 2-APB (100 μM) and $MgCl_2$ (10 mM) were very potent inhibitors, especially the latter. Of the TRPM7 inhibitors, NS8593 (10 μM) successfully inhibited the responses, but WA was not effective, although due to cell toxicity we only used low concentrations of it (5 μM). Altogether, the data suggest that besides $Ca_V3.2$, TRPM7 is an important contributor to Ca^{2+} influx in GV oocytes. We further confirmed this by demonstrating that Ca^{2+} influx in TRPV3-$Ca_V3.2$-KO oocytes is abrogated by treatment with the TRPM7 inhibitor NS8593 (10 μM) (Suppl. Fig. 4). These results are consistent with a recent report showing greatly reduced TG-induced Ca^{2+} influx in *Trpm7*-cKO GV oocytes [29,44,45].

3.3. Sr^{2+} induced oscillations in GV oocytes are greatly diminished in the absence of $Ca_V3.2$ channels

$[Sr^{2+}]_o$ was shown to generate action potentials in mouse MII eggs [17], and later studies showed that it is capable of inducing spontaneous oscillations in GV oocytes and MII eggs [12,46]. These oscillations likely represent, at least initially, intracellular changes in the concentrations of both Ca^{2+} and Sr^{2+}, although they are induced by the influx of Sr^{2+} from the extracellular media, which for these experiments is nominally Ca^{2+} free. However, the channel(s) responsible for mediating Sr^{2+} influx were unknown until recently when we showed TRPV3 mediates Sr^{2+} influx in MII eggs [27]. This study also reported that the functional expression of TRPV3 was low in GV oocytes, raising doubts whether it could mediate Sr^{2+} influx at this stage. We examined this question using *Trpv3*-KO GV oocytes, which showed robust Sr^{2+} oscillations, as we reported previously [28], although of lower frequency than WT oocytes (Fig. 5A, B, F; $P < 0.05$). Conversely, Sr^{2+} oscillations were severely curtailed in *$Ca_V3.2$*-KO, and almost absent in *Trpv3-$Ca_V3.2$*-KO oocytes suggesting that $Ca_V3.2$ channels play a pivotal role in mediating Sr^{2+} influx in GV oocytes (Fig. 5C-F; $P < 0.05$). Nevertheless, the fact that a few oscillations were still detectable in *Trpv3-$Ca_V3.2$*-KO oocytes suggests the presence of an additional channel(s).

To identify other channel(s) mediating Sr^{2+} influx in WT GV oocytes, we used the same series of pharmacological inhibitors. Consistent with genetic studies, the $Ca_V3.2$ inhibitors, mibefradil (1 μM) and Ni^{2+} (100 μM), immediately terminated Sr^{2+} oscillations in all treated oocytes (Fig. 6A-B). Among the broad-range inhibitors, $MgCl_2$ (10 mM) also immediately stopped the oscillations, although the non-specific inhibitor 2-APB (50 μM) only protractedly attenuated the oscillations (Fig. 6C). Remarkably, higher concentrations of 2-APB caused a large Sr^{2+} influx (100 μM, Suppl Fig. 5A-C), which is consistent with its role as an agonist of TRPV3 channels [47]; it also demonstrated for the first time functional expression, albeit incipient, of TRPV3 channels in GV oocytes. The inhibitors of TRPM7 channels showed dissimilar effects, as whereas addition of NS8593 (10 μM) terminated the oscillations after a short delay, WA (5 μM), the most specific TRPM7 inhibitor, was almost without effect (Fig. 6D). It is worth noting that we did not use inhibitors against TRPV3 channel in this study or throughout the manuscript, as none of the inhibitors tested blocked Sr^{2+} oscillations in MII eggs (data not shown). Collectively, our results show that $Ca_V3.2$ and to a lesser extent TRPV3 channels, contribute to Sr^{2+} influx in GV oocytes. The delayed inhibition of Sr^{2+} influx caused by NS8593, suggests this compound displays some off-target effects even when used at the recommended concentrations.

3.4. Mn^{2+} influx causes persistent quenching of Fura-2AM fluorescence

Mn^{2+} has long been used to study general pathways of divalent ion influx in cells, as its entry causes marked quenching of Fura-2 fluorescence that is easily detectable [48]. Mn^{2+} influx has been observed in both unfertilized and fertilized eggs [36], although the channel(s) that mediate(s) this influx remain(s) unknown. To address this question, we combined analysis of genetic KO models with results from pharmacological inhibitors. The addition of Mn^{2+} caused the expected quenching of Fura-2 fluorescence intensity in all oocytes, although the rate of decrease of the slope, assessed by percent of change in fluorescence, was reduced in *$Ca_V3.2$*-KO oocytes compared to WT, *Trpv3*-KO and *Trpv3-$Ca_V3.2$*-KO oocytes (Fig. 7A-D), suggesting that $Ca_V3.2$ channels are involved in Mn^{2+} influx at this stage. Remarkably, not only the rate of Mn^{2+} influx was increased in *Trpv3-$Ca_V3.2$*-KO oocytes, but also the

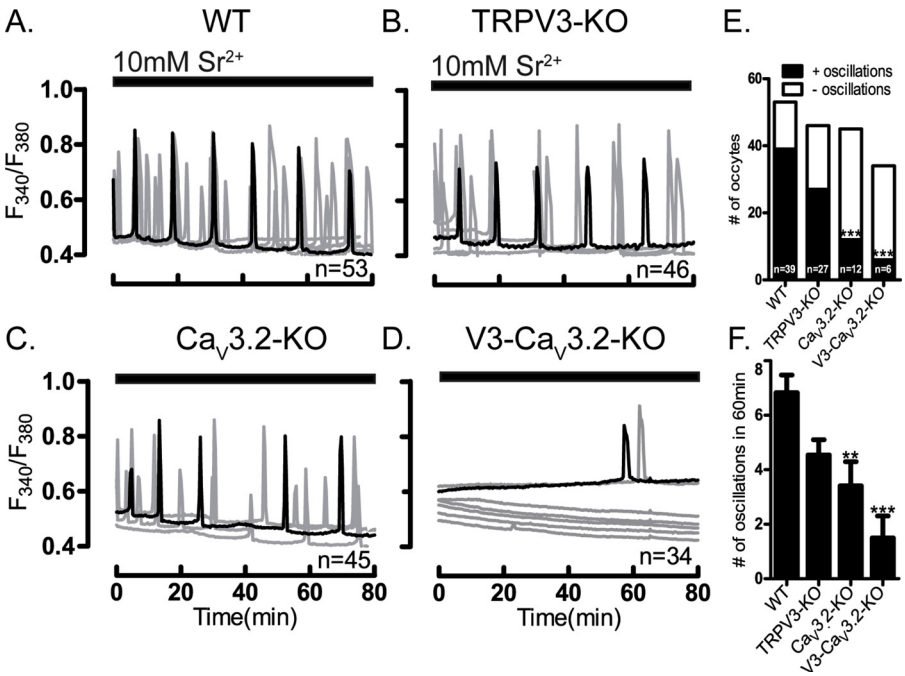

Fig. 5. Sr^{2+}-induced oscillations are diminished in *$Ca_V3.2$*- and *V3-$Ca_V3.2$*-KO oocytes. Sr^{2+} induced oscillations were tested in WT and in oocytes lacking TRPV3, or $Ca_V3.2$ or V3-$Ca_V3.2$ channels. Experiments were performed in nominal Ca^{2+}-free media containing 10 mM Sr^{2+}. **(A)** Sr^{2+} induced the expected oscillations in WT oocytes, and largely similar responses in **(B)** *TRPV3*-KO oocytes. Sr^{2+} induced oscillations were reduced in **(C)** *$Ca_V3.2$*-KO and in **(D)** *V3-$Ca_V3.2$*-KO oocytes both in the **(E)** number of cells showing oscillations, and in the **(F)** number of rises during the first 1 h of imaging ($P < 0.05$). Horizontal bars above each panel denote the time during which Sr^{2+} was present in the media. All experiments were performed in 3-4 replicates.

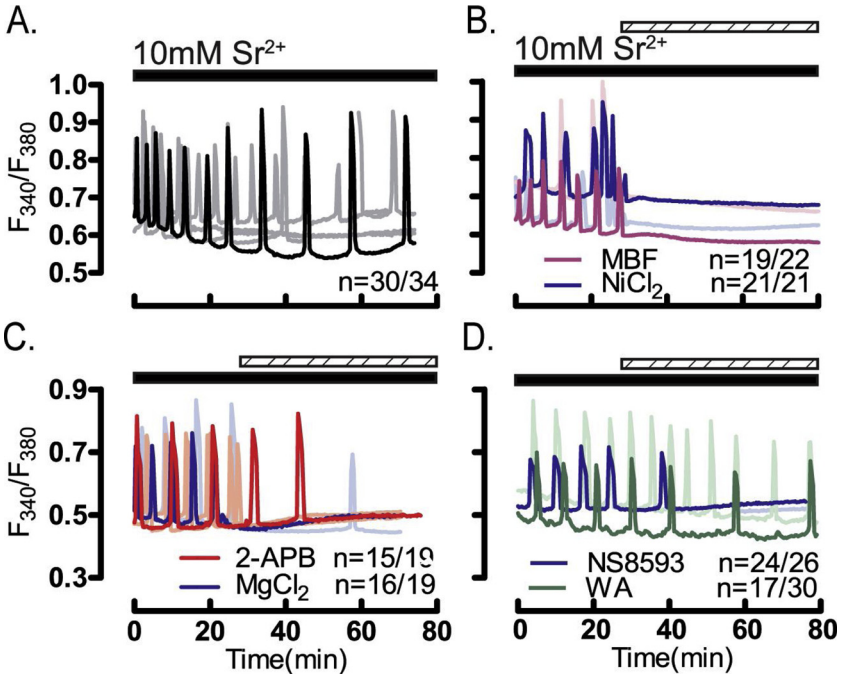

Fig. 6. $Ca_V3.2$ channels inhibitors rapidly terminate Sr^{2+} induced oscillations. Experiments were performed in nominal Ca^{2+}-free media containing 10 mM Sr^{2+} (black bar) and pharmacological inhibitors (dashed horizontal bars) were added 25 min following initiation of imaging. **(A)** Control, untreated oocytes showed normal oscillations, which were immediately terminated **(B)** by the addition of the $Ca_V3.2$ inhibitors MBF (1 μM) and Ni^{2+} (100 μM). **(C)** The general TRP channels inhibitors 2-APB (50 μM) & $MgCl_2$ (5 mM) and **(D)** the TRPM7 inhibitor NS8593 (10 μM) also terminated oscillations but more protractedly especially by the latter; waixenicin-A (5 μM) was without effect. All experiments were replicated 4 times.

time from addition to inflection was significantly shortened (Fig. 7E-F), suggesting that in these oocytes the expression of other channel(s) contributing to Mn^{2+} influx might be enhanced.

Further studies using mibefradil (1 μM) and Ni^{2+} (100 μM) confirmed the role of $Ca_V3.2$ channels, as they delayed and reduced the rate of fluorescence quenching compared to that of controls (Fig. 8A-B). 2-APB (50 μM) and $MgCl_2$ (10 mM) provided maximal inhibition, as they nearly eliminated influx, especially $MgCl_2$ (Fig. 8C), whereas TRPM7 inhibitors, delayed and reduced Mn^{2+} influx but did not abolish it (Fig. 8D). Altogether, these results suggest that Mn^{2+} influx in GV oocytes occurs through several channels mostly $Ca_V3.2$ [49] and TRPM7 [50], although their individual contributions still needs to be parsed out (Fig. 8E & F). The role of these channels was confirmed using NS8593 (10 μM) in TRPV3-$Ca_V3.2$-KO oocytes, which abrogated Mn^{2+} influx (Suppl. Fig. 6).

3.5. Ni^{2+} influx causes protracted and persistent quenching of Mag-Fura-2AM fluorescence

Ni^{2+} selectively blocks T-type channels [51] but is known to permeate other channels [30]. Ni^{2+} influx can be followed by the quenching it produces on the fluorescence of Fura-2 and Mag-Fura-2 [37,39,52]. We selected Mag-Fura-2 because is much less sensitive to the $[Ca^{2+}]_i$ increases induced by a variety of methods used in cells (Suppl. Fig. 7). Addition of Ni^{2+} caused a marked and comparable reduction in Mag-Fura-2 intensity in WT, *Trpv3*-KO and *$Ca_V3.2$*-KO oocytes suggesting that these channels are unlikely to participate in its influx (Fig. 9A-C). However, Ni^{2+} induced quenching was significantly increased in *Trpv3-$Ca_V3.2$*-KO oocytes (Fig. 9D-E), which is also reflected by the shortened time to inflection, implying that the responsible channel(s) permeating Ni^{2+} is still present in these KO

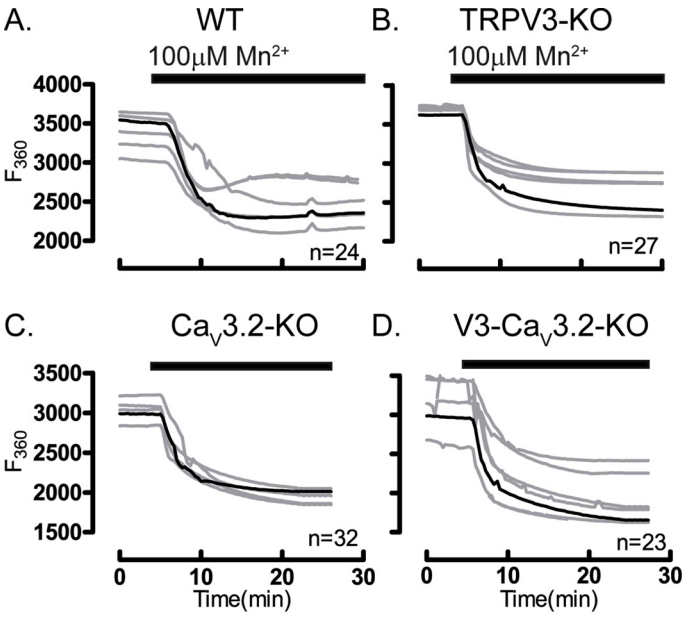

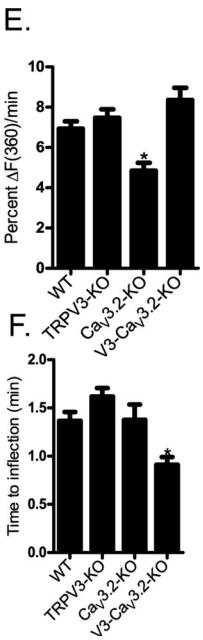

Fig. 7. Multiple channels enable Mn^{2+} entry. Mn^{2+} influx was tested in WT and in oocytes lacking TRPV3, or $Ca_V3.2$ or V3-$Ca_V3.2$ channels. Experiments were performed in media containing 2 mM Ca^{2+}. **(A)** Mn^{2+} influx in WT oocytes, **(B)** *TRPV3*-KO oocytes, **(C)** *$Ca_V3.2$*-KO oocytes, **(D)** *V3-$Ca_V3.2$*-KO oocytes. **(E)** Fluorescence quenching assessed by the rate of F360 nm fluorescence decrease per minute relative to baseline fluorescence ($P < 0.05$). **(F)** Time to inflection measured from the time of Mn^{2+} addition (5 min) to the time of first significant change in fluorescence values, which shortened in *V3-$Ca_V3.2$*-KO oocytes ($P < 0.05$). Black horizontal bars denote addition of 100 μM Mn^{2+}. Experiments were replicated 4 times.

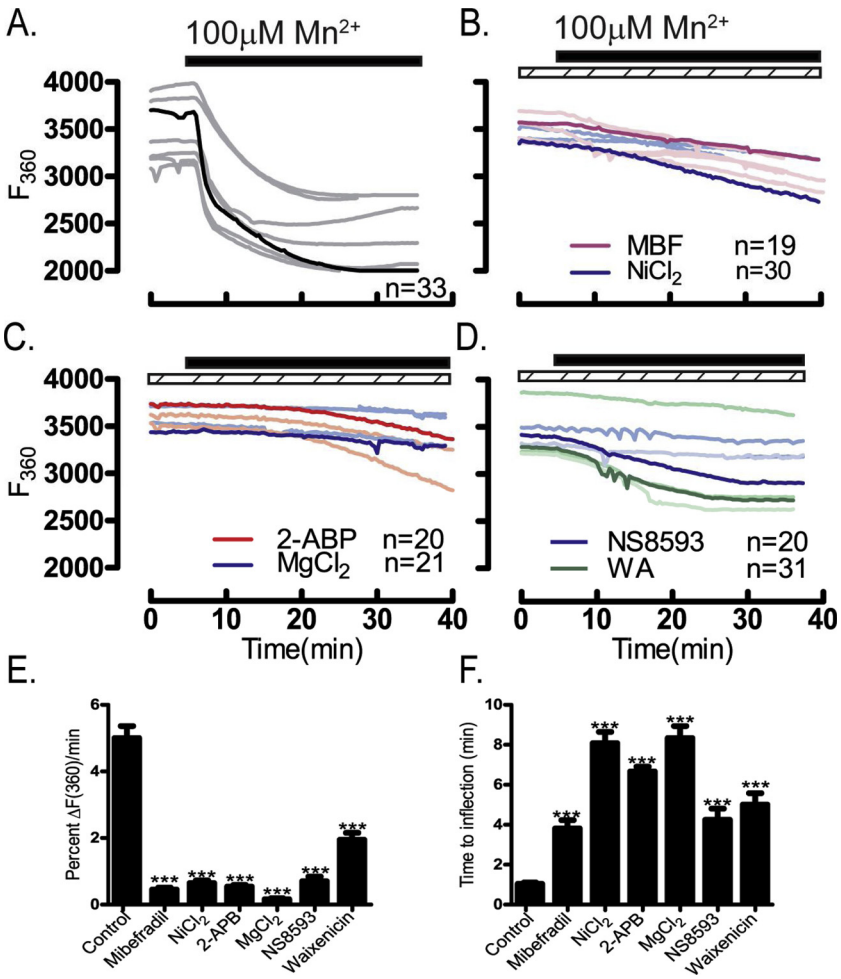

Fig. 8. Inhibitors of $Ca_V3.2$ & TRPM7 channels suppress Mn^{2+} influx. Mn^{2+} influx monitored using traces depicting quenching of F360 nm fluorescence. Experiments were performed in media containing 2 mM Ca^{2+} in the absence/presence of specific pharmacological inhibitors (dashed bars) after addition of Mn^{2+} (black bars): **(A)** control untreated oocytes, **(B)** oocytes treated with the $Ca_V3.2$ inhibitors MBF (1 μM) or Ni^{2+} (100 μM), **(C)** or with the general TRP inhibitors 2-APB (50 μM) and $MgCl_2$ (10 mM), or **(D)** with the TRPM7 inhibitors NS8593 (10 μM) or waixenicin-A (1 μM). **(E)** Rate of fluorescence quenching per minute at F360 nm relative to baseline fluorescence was reduced by all inhibitors examined ($P < 0.05$), and **(F)** time to inflection measured from the time of addition (5 min) to the time fluorescence quenching begins was prolonged by all inhibitors examined($P < 0.05$). Experiments were replicated 3 times.

oocytes (Fig. 9F). Our pharmacological studies showed that mibefradil (1 μM) had no effect on blocking Ni^{2+} influx (Fig. 10A, B) and that whereas both general inhibitors of TRP channels markedly reduced Ni^{2+} influx, $MgCl_2$ (10 mM) outperformed 2-APB (100 μM) (Fig. 10C). TRPM7 inhibitors abrogated Ni^{2+} influx, with NS8593 (10 μM) being the most potent of all inhibitors tested (Fig. 10D). Altogether, our

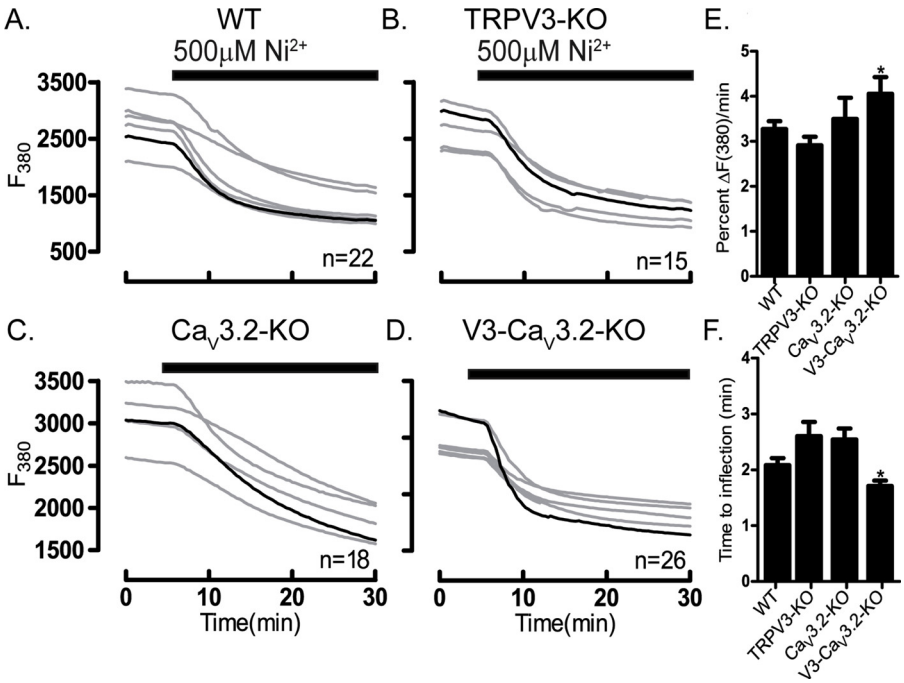

Fig. 9. Enhanced Ni^{2+} influx in *V3-$Ca_V3.2$*-KO oocytes. Ni^{2+} influx was tested in WT and oocytes lacking TRPV3, $Ca_V3.2$ or V3-$Ca_V3.2$ channels. Experiments were performed using Mag-Fura-2AM loaded oocytes in divalent free medium (DFM). Ni^{2+} influx in **(A)** WT oocytes, **(B)** *TRPV3*-KO oocytes, **(C)** *$Ca_V3.2$*-KO oocytes, **(D)** *V3-$Ca_V3.2$*-KO oocytes. **(E)** Fluorescence quenching at F380 assessed by the rate of fluorescence decrease per minute relative to baseline fluorescence ($*P < 0.05$). **(F)** Time to inflection measured from the time of addition (5 min) to the time fluorescence quenching begins ($*P < 0.05$). Black bars show the time at which Ni^{2+} was added. Experiments were replicated three times.

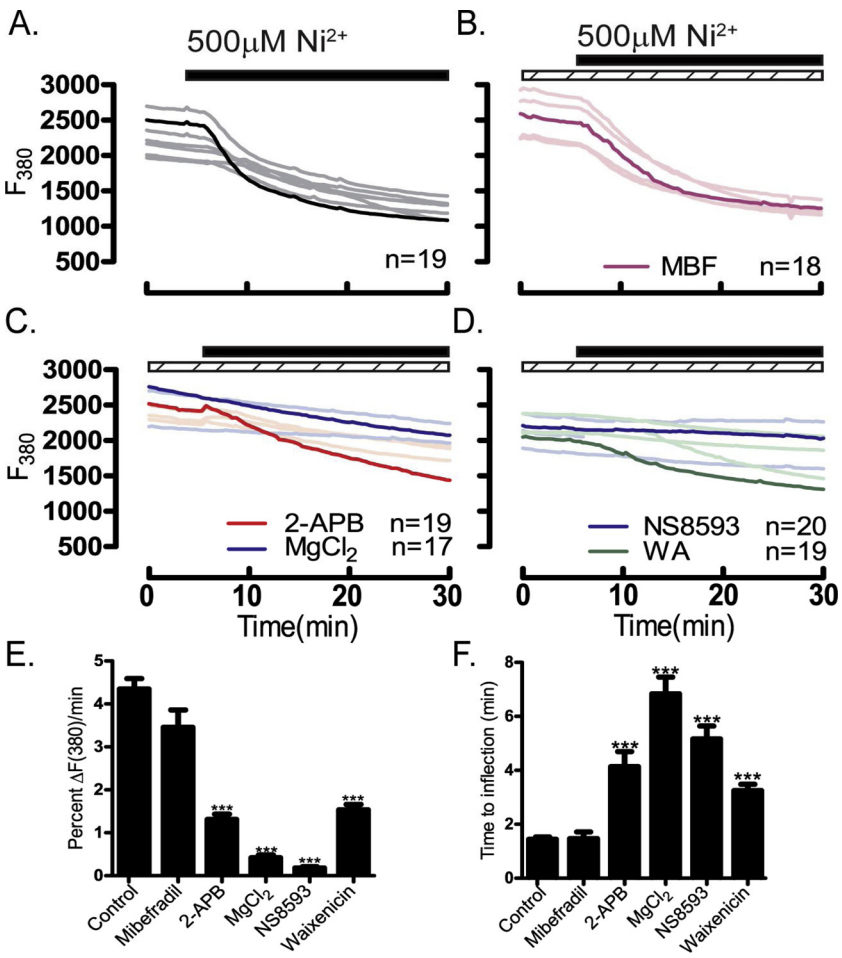

Fig. 10. TRPM7 channel inhibitors block Ni^{2+} influx. Inhibition of Ni^{2+} influx (black bars) was examined in the absence/presence of pharmacological inhibitors (dashed bars) and assessed by the rate of fluorescence quenching per minute at F380 relative to baseline fluorescence. Experiments were performed using Mag-Fura-2AM loaded oocytes in divalent free medium. **(A)** Control, untreated group, **(B)** $Ca_V3.2$ inhibitor MBF (1 μM), **(C)** general inhibitors of TRP channels 2-APB (100 μM) or $MgCl_2$ (10 mM), **(D)** TRPM7 inhibitors NS8593 (10 μM) or waixenicin-A (5 μM). **(E)** Maximal inhibition of fluorescence quenching of Mag-Fura by general TRP inhibitors, and more specifically by the TRPM7 inhibitor NS8593 ($P < 0.05$). **(F)** Time to inflection measured from the time of addition (5 min) to the time of fluorescence quenching begins, was also maximally inhibited by TRP inhibitors and more specifically by NS8593 ($P < 0.05$). Experiments were replicated 3 times.

results show that TRPM7 is likely to serve as the major pathway for Ni^{2+} influx in GV oocytes (Fig. 10E & F).

3.6. Different contribution of Ca^{2+} channels to the Ca^{2+} store content of GV oocytes

We next examined how the previously identified divalent cation permeable channels affect the intracellular Ca^{2+} content of GV oocytes. We used TG to evaluate the ER content in the null mouse lines described above. A significant reduction in the amplitude of the response was only observed in *$Ca_V3.2$*-KO oocytes (Fig. 11A & C), whereas the AUC measurements were not different for any of the groups ($P > 0.05$; data not shown). Similar results were obtained by Bernhardt et al., 2015 [21]. To measure total store content, we used IO in a similar cohort of oocytes. We found that the amplitude of the response was reduced in oocytes of all lines, but significantly in *Trpv3*- and *Trpv3-CaV3.2*-KO oocytes (Fig. 11B & D; $P < 0.05$), whereas the AUC response was reduced in all KO oocytes (Fig. 11E; $P < 0.05$).

We extended the above studies by incubating GV oocytes with the aforementioned inhibitors for 1 h, after which TG or IO was added and Ca^{2+} responses were monitored. The $Ca_V3.2$ inhibitors, mibefradil (1 μM) and Ni^{2+} (100 μM) significantly reduced the response to TG, and similar effects were observed in the presence of the general inhibitors 2-APB (100 μM) and $MgCl_2$ (10 mM) (Fig. 12A, B). The TRPM7 inhibitors were less effective (Fig. 12C). The responses to IO displayed a similar trend, with $Ca_V3.2$ inhibitors and general inhibitors providing the strongest inhibition, whereas the other inhibitors only displayed marginal effects, although NS8593 (10 μM) still reduced the amplitude of the response (Fig. 12, D–F). Altogether, these results reveal that under steady-state conditions, $Ca_V3.2$ channels are mostly responsible for the Ca^{2+} store content of GV oocytes, but contributions by TRPV3 and TRPM7 channels are also evident.

4. Discussion

In this study we examined the presence and function of channels that mediate divalent cation influx in mouse GV oocytes. We found that the three channels whose expression has been identified by electrophysiology in mouse oocytes and/or eggs are active at the GV stage. However, we observed that they respond distinctively to divalent cation exposure. We found for example that Ca^{2+} and Mn^{2+} influx is mostly dependent on $Ca_V3.2$ and TRPM7 channels, whereas Sr^{2+} induced oscillations largely rely on $Ca_V3.2$ expression and much less on TRPV3, and TRPM7 appears to mediate the totality of Ni^{2+} influx. Under steady-state conditions, $Ca_V3.2$ channels are primarily responsible for maintaining Ca^{2+} store content, although TRPM7 is able to mediate acute, induced Ca^{2+} influx demands. Lastly, as reported in other systems, broadly used inhibitors such as 2-APB and Ni^{2+} showed dual properties, as they effectively inhibited the influx of certain cations/channel(s), while simultaneously working as agonists for other channels; other inhibitors showed more uniform and specific effects. Identification of the channels responsible for Ca^{2+} and divalent cation homeostasis in GV oocytes and their molecular regulation during oocyte maturation could be used to improve fertility and also to prevent conception.

4.1. Non-selective channels mediate divalent cation influx in GV oocytes

The changes in Ca^{2+} homeostasis that occur in GV oocytes and the mechanisms that underpin them are less characterized than those in MII

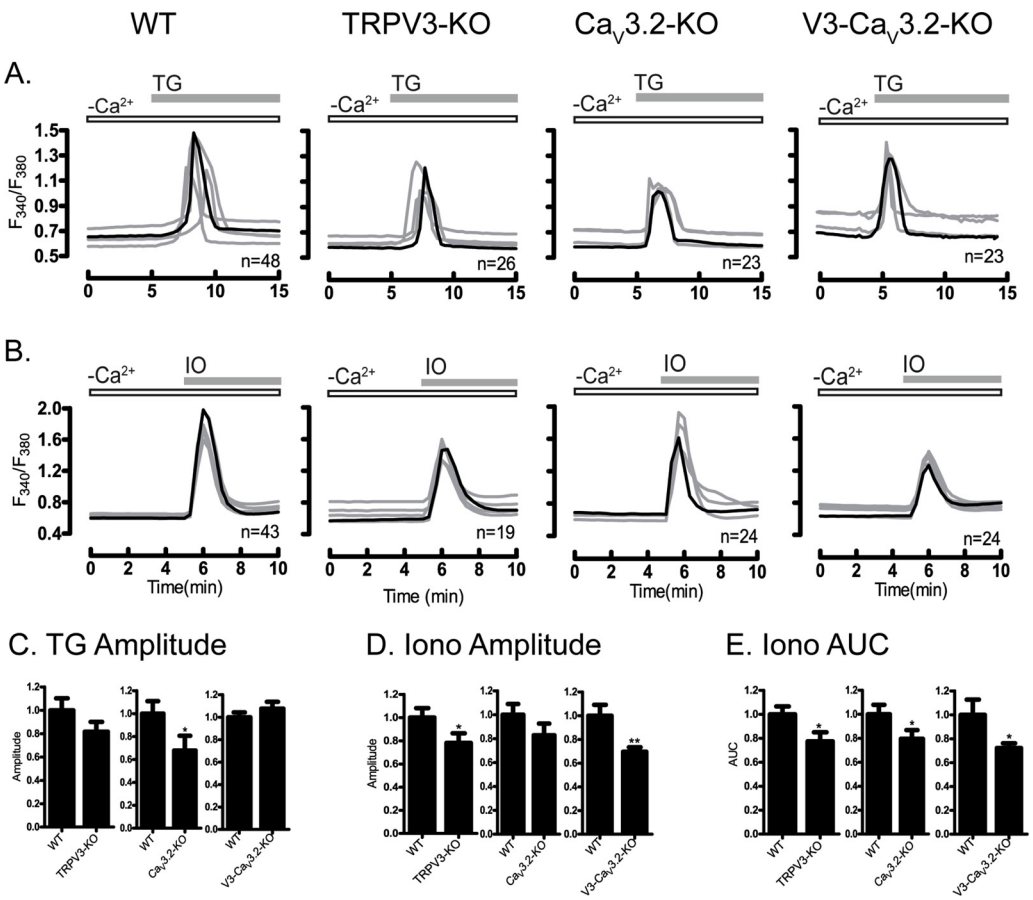

Fig. 11. The absence of TRPV3- and V3-Ca$_V$3.2 channels reduces internal Ca^{2+} stores. Ca^{2+} release from ER and total stores was measured using TG (10 μM) and IO (2.5 μM) in WT and in oocytes lacking TRPV3, Ca$_V$3.2, or V3-Ca$_V$3.2 channels. Experiments were performed in nominal Ca^{2+}-free medium. **(A)** TG responses in WT, *TRPV3-*, *Ca$_V$3.2-* and *V3-Ca$_V$3.2*-KO oocytes. **(B)** Ionomycin responses in WT, *TRPV3-*, *Ca$_V$3.2-* and *V3-Ca$_V$3.2*-KO oocytes. **(C)** Peak amplitude of TG-induced Ca^{2+} release was reduced in Ca$_V$3.2 ($P < 0.05$). **(D)** Peak amplitude of ionomycin-induced Ca^{2+} release was reduced V3-Ca$_V$3.2 ($P < 0.05$), whereas **(E)** AUC response induced by IO was reduced in all KO lines ($P < 0.05$). Open bars indicate nominal Ca^{2+} free media; filled gray bars show the time at which TG/IO was added. Experiments were replicated 3 times.

eggs. Not that they are less significant, as they contribute to maintain the mitochondrial function of these cells [53] as well as to increase the ER Ca^{2+} content during maturation [54]. Therefore, it is not surprising that several channels sustain Ca^{2+} influx at the GV stage. One of these channels is Ca$_V$3.2, which was recently suggested to be the sole functional T-type channel in mouse eggs [21]. Here, we found that oocytes from *Ca$_V$3.2* null mice failed to show the spontaneous oscillations that are stereotypical of this stage, a finding that was also replicated using specific inhibitors. Surprisingly, Ca^{2+} influx induced by increasing [Ca^{2+}]$_o$ or by re-addition of [Ca^{2+}]$_o$ after TG was only somewhat affected by the absence of Ca$_V$3.2 channels, and specific pharmacological inhibitors also caused modest inhibition of this influx. These results suggest that the expression of Ca$_V$3.2 channels mainly contributes to Ca^{2+} influx under basal, steady conditions whereas other channels, two of which are examined here, are capable of mediating Ca^{2+} influx when greater or acute demands of Ca^{2+} arise; these channels may maintain Ca^{2+} homeostasis in oocytes null for Ca$_V$3.2.

Consistent with the above results and with findings from the literature using heterologous expression and electrophysiology, Ca$_V$3.2 channels showed permeability to several divalent cations in the following order: $Mn^{2+} > Ca^{2+} > Sr^{2+}$. Therefore, it is not surprising that Ca$_V$3.2 channels appear indispensable for Sr^{2+} influx at the GV stage, which may be due in part to its higher permeability ratio for Sr^{2+} in relation to other cations [49]. It is intriguing nevertheless that despite the presence of Ca$_V$3.2 channels in mouse MII eggs [19,20,55], Sr^{2+} influx in these cells requires the expression of TRPV3 channels [27]. The difference between the GV and MII stages could be attributed to several factors such as higher expression of TRPV3 channels in MII eggs compared to Ca$_V$3.2, or an increase in the open probability of TRPV3 at the MII stage in relation to Ca$_V$3.2, or higher unitary conductance of TRPV3 channels for Sr^{2+} than Ca$_V$3.2 channels. These results raise the question of what regulates the expression and function of Ca$_V$3.2 channels in GV oocytes and throughout maturation. Whether or not these channels experience rearrangements in the channel pore that reshape the selectivity filter, as it is proposed to occur for certain channels [56], or are partly internalized [57], and/or differentially affect the function of neighboring channels or proteins during oocyte maturation will require additional investigation.

Another channel expressed in mouse oocytes and eggs is TRPV3 [27]. Remarkably, electrophysiological recordings and Ca^{2+} imaging studies in the presence of extracellular Ca^{2+} failed to detect functional expression of TRPV3 channels in GV oocytes [27]. Nevertheless, here using Sr^{2+}, 100 μM 2-APB and genetic models, we found that TRPV3 channels are functionally expressed in GV oocytes, although they are not the main mediators of Sr^{2+} influx at this stage, consistent with previous findings. The difference between our previous report and the present, is that the functional expression of TRPV3 in GV oocytes was tested by patch-clamping and imaging in the presence of Ca^{2+} but not of Sr^{2+} [27], which probably has a higher permeability ratio than Ca^{2+}. Further, in the present study, we estimated Sr^{2+} influx by monitoring Sr^{2+}-induced intracellular oscillations. These oscillations not only depend on the influx of Sr^{2+} across the membrane, but also rely on the modifications of IP$_3$R1 by Ca^{2+} or Sr^{2+}. Importantly, given that at the MII stage the sole mediator of Sr^{2+} influx and oscillations is TRPV3, and that its PM functional expression experiences a steady increase during maturation, future studies should examine the mechanism(s) regulating these changes.

We recently reported functional expression of a third channel in mouse oocytes and eggs, TRPM7 [28]. In that study we did not examine its role on Ca^{2+} influx or its impact on the content of the internal Ca^{2+} stores. This function however was addressed using a TRPM7 cKO line [29], which showed that cKO GV oocytes had comparable intracellular Ca^{2+} content to those of control eggs suggesting that TRPM7 channels are not responsible for the basal, steady Ca^{2+} influx. Remarkably,

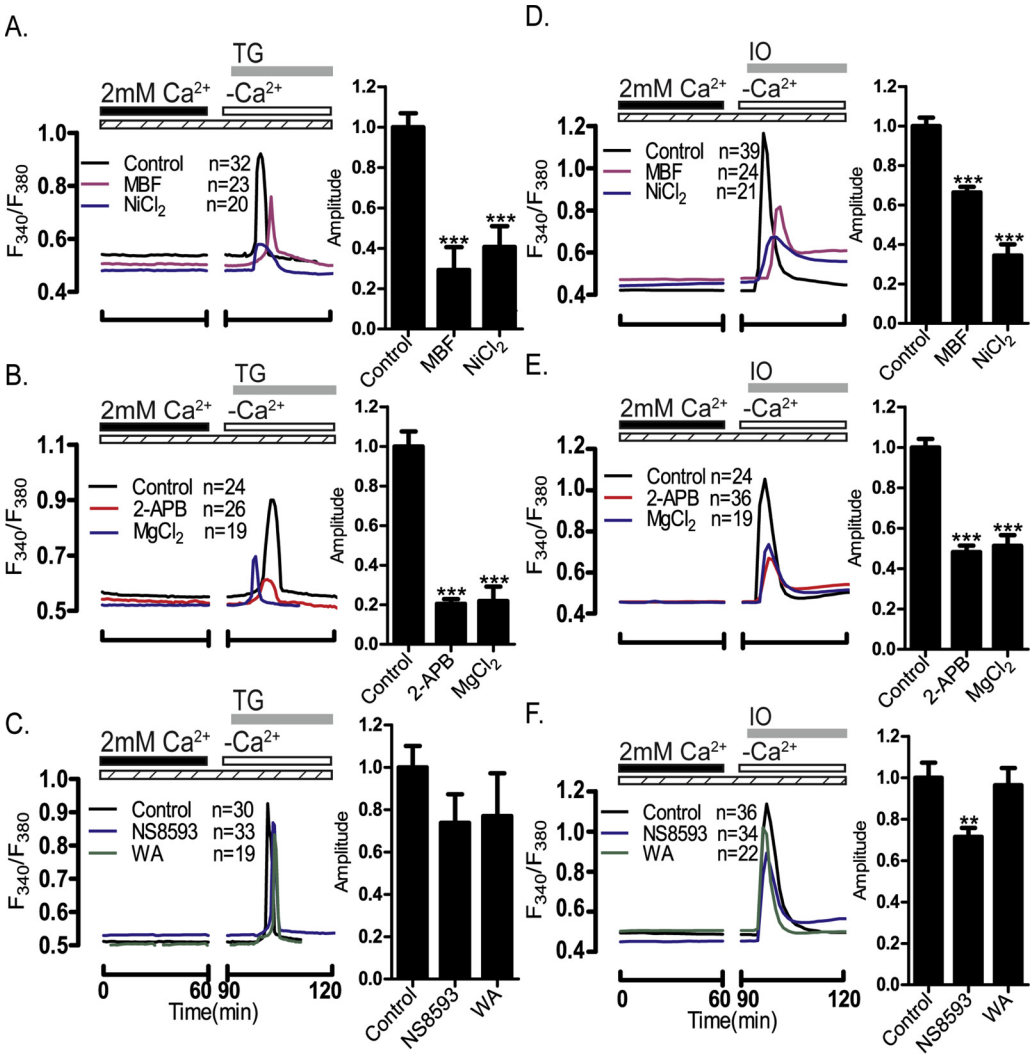

Fig. 12. Internal Ca^{2+} stores are reduced in the presence of $Ca_V3.2$ and general TRP channels inhibitors. Oocytes were incubated with pharmacological inhibitors for 1 h after which internal Ca^{2+} store content was tested following addition of TG and IO-induced. Peak amplitude of intracellular Ca^{2+} release was graphed and quantified. **(A and D)** the $Ca_V3.2$ inhibitors MBF (1 μM) and Ni^{2+} (100 μM) reduced responses to both treatments ($P < 0.05$), and similar effects were observed after the addition of **(B and E)** the TRP channels general inhibitors 2-APB (100 μM) and $MgCl_2$ (5 mM) ($P < 0.05$). **(C & F)** The TRPM7 inhibitors NS8593 (10 μM) & waixenicin-A (1 μM) were without effect ($P > 0.05$) regarding TG responses, while NS8593 affected the amplitude of the IO response ($P > 0.05$). Dashed bars indicate the presence of pharmacological inhibitors; black and white bars indicate the presence/absence of Ca^{2+}; gray bars show the time at which IO/TG was added.

TRPM7 cKO oocytes showed greatly reduced influx following addition of extra Ca^{2+} or re-addition of $[Ca^{2+}]_o$ after TG, which is indicative of the so-called SOCE mechanism [29]. Our findings with pharmacological inhibitors are consistent with these results, as the broad inhibitors, $MgCl_2$ and 2-APB, and also the TRPM7 inhibitors, NS8593 and WA, drastically reduced Ca^{2+} influx stimulated by TG exposure. It is worth noting that SOCE influx is usually mediated by the combined actions of Stim1 and Orai1 [58]. However, studies using GV oocytes from *Orai1*-KO or *Stim1/2*-cKO mice failed to show alterations of Ca^{2+} influx or spontaneous oscillations [24], which suggests that canonical SOCE might not play a significant role in mouse GV oocytes. Instead, TRPM7, which has been shown to modulate SOCE in lymphocytes [44,45], might be responsible for modulating acute Ca^{2+} influx and/or demands in GV oocytes. Future studies should ascertain the precise mechanism(s) of action whereby TRPM7 modulates this type of Ca^{2+} influx in GV oocytes as well as the influx of Ca^{2+} and other divalent cations during later stages of maturation, fertilization and early embryonic development. It is noteworthy that our western blotting results reveal possible phosphorylation of TRPM7 channels in mouse oocytes and eggs. It is well known that TRPM7 is phosphorylated in mammalian cells and it also undergoes autophosphorylation [59]. The effects of phosphorylation on TRPM7 are varied, and have been shown to alter the channel function as well as the stability and distribution of TRPM7 [60,61]. Future studies should examine the site(s) that are possibly modified in mouse oocytes and eggs and their impact on TRPM7 function(s).

The apparent minor role of TRPM7 in supporting basal Ca^{2+} influx in our study was also evidenced by the near absence of spontaneous Ca^{2+} oscillations in oocytes from *Trpv3-$Ca_V3.2$*-KO mice, where TRPM7 should feature prominently. Similarly, TRPM7 did not appear to support steady Sr^{2+}influx in GV oocytes, as *Trpv3-$Ca_V3.2$*-KO oocytes display greatly reduced oscillations in its presence. The TRPM7-like channel nevertheless mediated Mn^{2+} influx, and it appears to be the sole mediator of Ni^{2+} influx, which is consistent with its known permeability ratio to Ca^{2+} from electrophysiological studies in somatic cells [30]. Consistent with this, the influx of Mn^{2+} and Ni^{2+} was only somewhat decreased in oocytes of single channel KO lines, and it was enhanced in *Trpv3-$Ca_V3.2$*-KO oocytes. Lastly, Mn^{2+} and Ni^{2+} influx were abrogated by NS8593 and greatly diminished by WA – the more specific of the TRPM7 inhibitors [43]. Our results therefore suggest that although TRPM7 channels do not contribute to steady-state Ca^{2+} influx in GV oocytes, at least under our conditions that contained $[Mg^{2+}]_o$, they may play an important role when abrupt Ca^{2+} demands arise. TRPM7 channels might also mediate the influx of other divalent cations such as Zn^{2+}, Co^{2+} and Mg^{2+}, which are all important enzyme-cofactors [62], and in the case of Zn^{2+} is also important for post-implantation embryo development [63]. Future studies should determine whether the early embryonic lethality associated with the loss of TRPM7 is due to reduced Ca^{2+} influx or reflects a combined deficiency in the influx of one or more of the aforementioned divalent cations. Indeed, genetic ablation of the channel function of TRPM7 in the intestine impacts the homeostasis of Zn^{2+}, Mg^{2+}, and Ca^{2+} at the organismal level leading to deficiencies that are incompatible with post-

natal survival [64].

4.2. Ca^{2+} influx and store content in GV oocytes

The increase in the content of the internal Ca^{2+} stores throughout oocyte maturation is a well-documented phenomenon [2,8,65]. In GV oocytes, the internal Ca^{2+} stores contain low Ca^{2+}, and the content remains low even if oocytes are arrested at this stage for prolonged periods of time, which is all the most remarkable because it happens despite persistent Ca^{2+} influx [10]. Importantly, GV oocytes contain some Ca^{2+} in the stores and if one of the channels under consideration here, or if other undiscovered channel(s) contribute to their filling is not presently known. Recent studies used genetic models to address this question. Unexpectedly, it was found that oocytes lacking the molecular components of SOCE showed unaltered store content [24], and the same conclusion was drawn from studies using TRPM7 cKO oocytes [29]. Conversely, the Ca^{2+} store of oocytes lacking $Ca_V3.2$ was unevenly affected, although the TG- sensitive stores were reduced, the total Ca^{2+} store content as assessed by IO was unaffected [21]. In the present study, we found that absence of $Ca_V3.2$ channels diminished both the TG-sensitive stores and the total stores, whereas the absence of *Trpv3*-KO channels reduced the total store content. Consistent with these results, simultaneous deletion of *$Ca_V3.2$* and *Trpv3* synergistically diminished total store content, findings that were largely replicated by the addition of pharmacological inhibitors. Of these, the general and $Ca_V3.2$ channel-specific inhibitors maximally reduced Ca^{2+} store content, whereas TRPM7 inhibitors had lesser impact, findings that are consistent with a published genetic study [29]. In those studies, simultaneous deletion of $Ca_V3.2$ and TRPM7 channels synergistically reduced TG-sensitive stores in MII eggs and the number of pups per litter [29]. Together, our studies show that despite functional expression of at least three divalent cation permeable channels on the PM of GV oocytes, these channels contribute distinctly to the filling of the internal stores. Future studies should examine why and how this is determined, and whether the distribution of these channels on the PM and/or their relationship to the ER organization impacts the contribution to the filling of the stores at the GV stage and during maturation.

4.3. Ca^{2+} channel inhibitors in GV oocytes

Although inhibitors of PM channels have been used for decades to identify Ca^{2+} channels and their functions in neurons and other somatic cells [37], the use of these blockers in mammalian oocytes and eggs has been limited. Here we employ a combination of inhibitors to identify the expression and contribution of PM channels to the Ca^{2+} homeostasis of GV oocytes. Further, because we contrasted their effectiveness with cation influx in oocytes null for two of these channels, we can make inferences about their specificity. Of the two broad inhibitors used, $MgCl_2$ seemed to be the ideal compound, as it affects the conduction properties of all the three channels whose expression is known in oocytes and eggs [66,67]. Consistent with these reports, 10 mM Mg^{2+} effectively blocked influx of all divalent cations examined, although a range of concentrations would be necessary to determine if differential sensitivity to it exists among these channels. The other broad inhibitor, 2-APB, produced less consistent responses, as it effectively inhibited Ca^{2+} influx at all concentrations, while at higher concentrations acted as a TRPV3 agonist promoting Sr^{2+} influx [47]. Thus, 2-APB has disparate effects on divalent cation influx in GV oocytes that depends on the concentration of the drug, as it was reported in somatic cells, and the divalent cation under consideration. The inhibitors of $Ca_V3.2$ channels also produced some unexpected results. While 1 μM mibefradil consistently inhibited the influx of Ca^{2+}, Sr^{2+} and Mn^{2+}, 100 μM Ni^{2+} did not attenuate Ca^{2+} influx when promoted by addition of extra Ca^{2+} or following re-addition of Ca^{2+} after TG. These results are consistent with Ni^{2+}'s high permeability through TRPM7 [30], which may also be relieving the block in TRPM7's pore region induced by Ca^{2+} and/or Mg^{2+} [30], causing Ca^{2+} to permeate this channel as well as other present active channel(s) more effectively. Thus, the Ca^{2+} responses after the addition of Ni^{2+} should be interpreted with caution, as its presence simultaneously inverses the functional activity of two channels expressed in mouse oocytes and eggs. Both TRPM7 inhibitors used here proved effective at blocking TRPM7-like channels, although WA was the most specific, as it blocked Ni^{2+} influx and curtailed stimulated Ca^{2+} influx without affecting Sr^{2+} influx; we could not test the full effectiveness of WA, as the concentrations recommended in somatic cells of ~10 μM [43] proved toxic for GV oocytes. NS8593 displayed stronger inhibitory properties, although it also protractedly inhibited Sr^{2+} influx suggesting residual effects on $Ca_V3.2$ channels, which may explain its stronger effect on the content of the internal Ca^{2+} stores.

4.4. Conclusions

In conclusion, we show that divalent cations permeate GV oocytes through at least three different channels. These channels are all non-selective, although they might display different permeability ratios for the ions tested here. Similarly, we found these channels differentially contribute to the constitutive, steady-state Ca^{2+} influx vs. stimulated Ca^{2+} influx, and to the filling of internal Ca^{2+} stores, although the underlying cellular and/or molecular reasons behind these differences are unknown. Lastly, we characterized inhibitors and concentrations that can reliably prevent influx of specific divalent cations and identified the agonist properties of other inhibitors. Future studies should examine how changes in Ca^{2+} homeostasis at the GV stage impact maturation and oocyte developmental competence.

Footnotes

The content is solely the responsibility of the authors and doesn't necessarily represent the official views of the National Institute of Health.

Declaration of Competing Interest

None.

Acknowledgments

This study was supported in part by a NIH grant (NICHD092499) to R.A.F. G.A. was supported in part by the Frances and Chou-Chu Hong Graduate Fellowship in Veterinary and Animal Sciences, UMass Amherst. The work in the labortatory of F.D.H. to purify WA was supported by a grant from NIH NIGMS P20GM103466. We thank Banyoon Cheon for technical assistance in primers design and Changli He for overall technical support.

Appendix A. Supplementary data

Supplementary material related to this article can be found, in the online version, at doi:https://doi.org/10.1016/j.ceca.2020.102181.

References

[1] M.J. Berridge, P. Lipp, M.D. Bootman, The versatility and universality of calcium signalling, Nat. Rev. Mol. Cell Biol. 1 (1) (2000) 11–21.
[2] T. Wakai, V. Vanderheyden, R.A. Fissore, Ca2+ signaling during mammalian fertilization: requirements, players, and adaptations, Cold Spring Harb. Perspect. Biol. 3 (4) (2011).
[3] K.S. Cuthbertson, D.G. Whittingham, P.H. Cobbold, Free Ca2+ increases in exponential phases during mouse oocyte activation, Nature 294 (5843) (1981) 754–757.
[4] E.B. Ridgway, J.C. Gilkey, L.F. Jaffe, Free calcium increases explosively in activating medaka eggs, Proc. Natl. Acad. Sci. U. S. A. 74 (2) (1977) 623–627.
[5] R. Steinhardt, R. Zucker, G. Schatten, Intracellular calcium release at fertilization in the sea urchin egg, Dev. Biol. 58 (1) (1977) 185–196.

[6] S.A. Stricker, Comparative biology of calcium signaling during fertilization and egg activation in animals, Dev. Biol. 211 (2) (1999) 157–176.
[7] J. Carroll, K. Swann, Spontaneous cytosolic calcium oscillations driven by inositol trisphosphate occur during in vitro maturation of mouse oocytes, J. Biol. Chem. 267 (16) (1992) 11196–11201.
[8] K.T. Jones, J. Carroll, D.G. Whittingham, Ionomycin, thapsigargin, ryanodine, and sperm induced Ca2+ release increase during meiotic maturation of mouse oocytes, J. Biol. Chem. 270 (12) (1995) 6671–6677.
[9] R.M. Tombes, et al., Meiosis, egg activation, and nuclear envelope breakdown are differentially reliant on Ca2+, whereas germinal vesicle breakdown is Ca2+ independent in the mouse oocyte, J. Cell Biol. 117 (4) (1992) 799–811.
[10] B. Cheon, et al., Ca2+ influx and the store-operated Ca2+ entry pathway undergo regulation during mouse oocyte maturation, Mol. Biol. Cell 24 (9) (2013) 1396–1410.
[11] T. Wakai, et al., Regulation of endoplasmic reticulum Ca(2+) oscillations in mammalian eggs, J. Cell. Sci. 126 (Pt 24) (2013) 5714–5724.
[12] D. Kline, J.T. Kline, Thapsigargin activates a calcium influx pathway in the unfertilized mouse egg and suppresses repetitive calcium transients in the fertilized egg, J. Biol. Chem. 267 (25) (1992) 17624–17630.
[13] D.E. Clapham, Calcium signaling, Cell 131 (6) (2007) 1047–1058.
[14] S. Hagiwara, S. Miyazaki, Ca and Na spikes in egg cell membrane, Prog. Clin. Biol. Res. 15 (1977) 147–158.
[15] J.M. Murnane, L.J. DeFelice, Electrical maturation of the murine oocyte: an increase in calcium current coincides with acquisition of meiotic competence, Zygote 1 (1) (1993) 49–60.
[16] A. Peres, Resting membrane potential and inward current properties of mouse ovarian oocytes and eggs, Pflugers Arch. 407 (5) (1986) 534–540.
[17] S. Yoshida, Permeation of divalent and monovalent cations through the ovarian oocyte membrane of the mouse, J. Physiol. 339 (1983) 631–642.
[18] W.A. Catterall, Structure and regulation of voltage-gated Ca2+ channels, Annu. Rev. Cell Dev. Biol. 16 (2000) 521–555.
[19] M.L. Day, M.H. Johnson, D.I. Cook, Cell cycle regulation of a T-type calcium current in early mouse embryos, Pflugers Arch. 436 (6) (1998) 834–842.
[20] D. Kang, et al., Acetylcholine increases Ca2+ influx by activation of CaMKII in mouse oocytes, Biochem. Biophys. Res. Commun. 360 (2) (2007) 476–482.
[21] M.L. Bernhardt, et al., CaV3.2 T-type channels mediate Ca(2)(+) entry during oocyte maturation and following fertilization, J. Cell. Sci. 128 (23) (2015) 4442–4452.
[22] C. Gomez-Fernandez, et al., Calcium signaling in mouse oocyte maturation: the roles of STIM1, ORAI1 and SOCE, Mol. Hum. Reprod. 18 (4) (2012) 194–203.
[23] Z. Machaty, et al., Fertility: store-operated Ca(2+) entry in germ cells: role in egg activation, Adv. Exp. Med. Biol. 993 (2017) 577–593.
[24] M.L. Bernhardt, et al., Store-operated Ca(2+) entry is not required for fertilization-induced Ca(2+) signaling in mouse eggs, Cell Calcium 65 (2017) 63–72.
[25] B.N. Desai, D.E. Clapham, TRP channels and mice deficient in TRP channels, Pflugers Arch. 451 (1) (2005) 11–18.
[26] L.J. Wu, T.B. Sweet, D.E. Clapham, International Union of Basic and Clinical Pharmacology. LXXVI. Current progress in the mammalian TRP ion channel family, Pharmacol. Rev. 62 (3) (2010) 381–404.
[27] I. Carvacho, et al., TRPV3 channels mediate strontium-induced mouse-egg activation, Cell Rep. 5 (5) (2013) 1375–1386.
[28] I. Carvacho, et al., TRPM7-like channels are functionally expressed in oocytes and modulate post-fertilization embryo development in mouse, Sci. Rep. 6 (2016) 34236.
[29] M.L. Bernhardt, et al., TRPM7 and CaV3.2 channels mediate Ca(2+) influx required for egg activation at fertilization, Proc. Natl. Acad. Sci. U. S. A. 115 (44) (2018) E10370–E10378.
[30] M.K. Monteilh-Zoller, et al., TRPM7 provides an ion channel mechanism for cellular entry of trace metal ions, J. Gen. Physiol. 121 (1) (2003) 49–60.
[31] B.Y. Kong, et al., Zinc maintains prophase I arrest in mouse oocytes through regulation of the MOS-MAPK pathway, Biol. Reprod. 87 (1) (2012) 1–12 p. 11.
[32] C.C. Chen, et al., Abnormal coronary function in mice deficient in alpha1H T-type Ca2+ channels, Science 302 (5649) (2003) 1416–1418.
[33] X. Cheng, et al., TRP channel regulates EGFR signaling in hair morphogenesis and skin barrier formation, Cell 141 (2) (2010) 331–343.
[34] H.C. Lee, et al., TRPV3 channels mediate Ca(2)(+) influx induced by 2-APB in mouse eggs, Cell Calcium 59 (1) (2016) 21–31.
[35] D. Zhang, et al., Strontium promotes calcium oscillations in mouse meiotic oocytes and early embryos through InsP3 receptors, and requires activation of phospholipase and the synergistic action of InsP3, Hum. Reprod. 20 (11) (2005) 3053–3061.
[36] T.R. Cheek, et al., Fertilisation and thimerosal stimulate similar calcium spiking patterns in mouse oocytes but by separate mechanisms, Development 119 (1) (1993) 179–189.
[37] J.E. Merritt, R. Jacob, T.J. Hallam, Use of manganese to discriminate between calcium influx and mobilization from internal stores in stimulated human neutrophils, J. Biol. Chem. 264 (3) (1989) 1522–1527.
[38] J.H. Lee, et al., Nickel block of three cloned T-type calcium channels: low concentrations selectively block alpha1H, Biophys. J. 77 (6) (1999) 3034–3042.
[39] M. Tashiro, H. Inoue, M. Konishi, Physiological pathway of magnesium influx in rat ventricular myocytes, Biophys. J. 107 (9) (2014) 2049–2058.
[40] G.S. Bird, et al., Methods for studying store-operated calcium entry, Methods 46 (3) (2008) 204–212.
[41] C. McCloskey, et al., Voltage-dependent Ca2+ currents contribute to spontaneous Ca2+ waves in rabbit corpus cavernosum myocytes, J. Sex. Med. 6 (11) (2009) 3019–3031.
[42] V. Chubanov, et al., Natural and synthetic modulators of SK (K(ca)2) potassium channels inhibit magnesium-dependent activity of the kinase-coupled cation channel TRPM7, Br. J. Pharmacol. 166 (4) (2012) 1357–1376.
[43] S. Zierler, et al., Waixenicin A inhibits cell proliferation through magnesium-dependent block of transient receptor potential melastatin 7 (TRPM7) channels, J. Biol. Chem. 286 (45) (2011) 39328–39335.
[44] P. Beesetty, et al., Inactivation of TRPM7 kinase in mice results in enlarged spleens, reduced T-cell proliferation and diminished store-operated calcium entry, Sci. Rep. 8 (1) (2018) 3023.
[45] M. Faouzi, et al., The TRPM7 channel kinase regulates store-operated calcium entry, J. Physiol. 595 (10) (2017) 3165–3180.
[46] A. Bos-Mikich, K. Swann, D.G. Whittingham, Calcium oscillations and protein synthesis inhibition synergistically activate mouse oocytes, Mol. Reprod. Dev. 41 (1) (1995) 84–90.
[47] H.Z. Hu, et al., 2-aminoethoxydiphenyl borate is a common activator of TRPV1, TRPV2, and TRPV3, J. Biol. Chem. 279 (34) (2004) 35741–35748.
[48] D. Luo, et al., Signaling pathways underlying muscarinic receptor-induced [Ca2+]i oscillations in HEK293 cells, J. Biol. Chem. 276 (8) (2001) 5613–5621.
[49] T. Kaku, et al., The gating and conductance properties of Cav3.2 low-voltage-activated T-type calcium channels, Jpn. J. Physiol. 53 (3) (2003) 165–172.
[50] M. Li, J. Jiang, L. Yue, Functional characterization of homo- and heteromeric channel kinases TRPM6 and TRPM7, J. Gen. Physiol. 127 (5) (2006) 525–537.
[51] A. Bhattacharjee, et al., T-type calcium channels facilitate insulin secretion by enhancing general excitability in the insulin-secreting beta-cell line, INS-1, Endocrinology 138 (9) (1997) 3735–3740.
[52] M.V. Golynskiy, et al., Metal binding studies and EPR spectroscopy of the manganese transport regulator MntR, Biochemistry 45 (51) (2006) 15359–15372.
[53] T. Wakai, R.A. Fissore, Constitutive IP3R1-mediated Ca(2+) release reduces Ca(2+) store content and stimulates mitochondrial metabolism in mouse GV oocytes, J. Cell. Sci. 132 (3) (2019).
[54] K.T. Jones, V.L. Nixon, Sperm-induced Ca(2+) oscillations in mouse oocytes and eggs can be mimicked by photolysis of caged inositol 1,4,5-trisphosphate: evidence to support a continuous low level production of inositol 1, 4,5-trisphosphate during mammalian fertilization, Dev. Biol. 225 (1) (2000) 1–12.
[55] A. Peres, The calcium current of mouse egg measured in physiological calcium and temperature conditions, J. Physiol. (Paris) 391 (1987) 573–588.
[56] B.S. Khakh, H.A. Lester, Dynamic selectivity filters in ion channels, Neuron 23 (4) (1999) 653–658.
[57] A.K. Shukla, et al., Arresting a transient receptor potential (TRP) channel: beta-arrestin 1 mediates ubiquitination and functional down-regulation of TRPV4, J. Biol. Chem. 285 (39) (2010) 30115–30125.
[58] J.T. Smyth, et al., Activation and regulation of store-operated calcium entry, J. Cell. Mol. Med. 14 (10) (2010) 2337–2349.
[59] T.Y. Kim, et al., Identification of the phosphorylation sites on intact TRPM7 channels from mammalian cells, Biochem. Biophys. Res. Commun. 417 (3) (2012) 1030–1034.
[60] N. Cai, et al., The kinase activity of the channel-kinase protein TRPM7 regulates stability and localization of the TRPM7 channel in polarized epithelial cells, J. Biol. Chem. 293 (29) (2018) 11491–11504.
[61] C. Schmitz, et al., The channel kinases TRPM6 and TRPM7 are functionally nonredundant, J. Biol. Chem. 280 (45) (2005) 37763–37771.
[62] M.J. Knape, et al., Divalent metal ions control activity and inhibition of protein kinases, Metallomics 9 (11) (2017) 1576–1584.
[63] X. Tian, et al., Preconception zinc deficiency disrupts postimplantation fetal and placental development in mice, Biol. Reprod. 90 (4) (2014) 83.
[64] L. Mittermeier, et al., TRPM7 is the central gatekeeper of intestinal mineral absorption essential for postnatal survival, Proc. Natl. Acad. Sci. U. S. A. (2019).
[65] L.M. Mehlmann, D. Kline, Regulation of intracellular calcium in the mouse egg: calcium release in response to sperm or inositol trisphosphate is enhanced after meiotic maturation, Biol. Reprod. 51 (6) (1994) 1088–1098.
[66] J. Luo, et al., Tonic inhibition of TRPV3 by Mg2+ in mouse epidermal keratinocytes, J. Invest. Dermatol. 132 (9) (2012) 2158–2165.
[67] P. Demeuse, R. Penner, A. Fleig, TRPM7 channel is regulated by magnesium nucleotides via its kinase domain, J. Gen. Physiol. 127 (4) (2006) 421–434.